Z. Phys. C – Particles and Fields 32, 11–19 (1986)

Zeitschrift für Physik C Particles and Fields

Vector Meson Production in the Final State $K^+K^-\pi^+\pi^-$ of Photon-Photon Collisions

TASSO Collaboration

M. Althoff[1], W. Braunschweig, R. Gerhards, J.F. Kirschfink, H.-U. Martyn, P. Rosskamp, W. Wallraff

I. Physikalisches Institut der RWTH Aachen, D-5100 Aachen, Federal Republic of Germany[15]

B. Bock, J. Eisenmann, H.M. Fischer, H. Hartmann, A. Jocksch, H. Kolanoski, H. Kück[2], V. Mertens, R. Wedemeyer

Physikalisches Institut der Universität Bonn, D-5300 Bonn, Federal Republic of Germany[15]

B. Foster

H.H. Wills Physics Laboratory, University of Bristol, Bristol BS8 1TL, UK[16]

E. Bernardi, Y. Eisenberg[3], A. Eskreys[4], K. Gather, H. Hultschig, P. Joos, B. Klima, H. Kowalski, A. Ladage, B. Löhr, D. Lüke, P. Mättig[5], D. Notz, D. Revel[3], E. Ronat[3], D. Trines, T. Tymieniecka[6], R. Walczak[7], G. Wolf, W. Zeuner

Deutsches Elektronen-Synchrotron, DESY, D-2000 Hamburg, Federal Republic of Germany

E. Hilger T. Kracht, H.L. Krasemann[8], J. Krüger, E. Lohrmann, G. Poelz, K.-U. Pösnecker

II. Institut für Experimentalphysik der Universität Hamburg, D-2000 Hamburg, Federal Republic of Germany[15]

D.M. Binnie, P. Dornan, D.A. Garbutt, C. Jenkins, W.G. Jones, J.K. Sedgbeer, D. Su, J. Thomas[9], W.A.T. Wan Abdullah[10]

Department of Physics, Imperial College, London SW7 2AZ, UK[16]

F. Barreiro, E. Ros

Universidad Autonoma de Madrid, Madrid, Spain[19]

M.G. Bowler, P. Bull, R.J. Cashmore, P. Dauncey, R. Devenish, G. Heath, D.J. Mellor, P. Ratoff

Department of Nuclear Physics, Oxford University, Oxford, UK[16]

S.L. Lloyd

Department of Physics, Queen Mary College, London E1 4NS, UK[16]

K. Bell, G.E. Forden, J.C. Hart, D.K. Hasell, D.H. Saxon

Rutherford Appleton Laboratory, Chilton, Didcot, Oxon OX11 OQX, UK[16]

S. Brandt, M. Holder, L. Labarga[11], B. Neumann

Fachbereich Physik der Universität-Gesamthochschule Siegen, D-5900 Siegen, Federal Republic of Germany[15]

U. Karshon, G. Mikenberg, A. Montag, R. Mir, E. Duchovni, A. Shapira, G. Yekutieli

Weizmann Institute, Rehovot 76100, Israel[17]

G. Baranko, A. Caldwell, M. Cherney[12], J.M. Izen[13], S. Ritz, D. Strom, M. Takashima, E. Wicklund[14], Sau Lan Wu, G. Zobernig

Department of Physics, University of Wisconsin, Madison, WI 53706, USA[18]

Received 11 March 1986

[1] Now at Siemens, München, FRG
[2] Now at Fraunhofer Institut, Duisburg, FRG
[3] On leave from Weizmann Institute, Rehovot, Israel
[4] On leave from Institute of Nuclear Physics, Cracow, Poland
[5] Now at IPP Canada, Carleton Univeristy, Ottawa, Canada
[6] Now at Warsaw University, Poland
[7] On leave from Warsaw University, Poland
[8] Now at GKSS, Geesthacht, FRG
[9] Now at CERN, Geneva, Switzerland
[10] Now at University of Malaya, Kuala Lumpur, Malaysia
[11] On leave from Universidad Autonomia de Madrid, Madrid, Spain
[12] Now at Lawrence Berkeley Laboratory, Berkeley, CA, USA
[13] Now at University of Illinois at Urbana-Champaign, Urbana, IL, USA
[14] Now at California Institute of Technology, Pasadena, CA, USA
[15] Supported by the Bundesministerium für Forschung und Technologie
[16] Supported by the UK Science and Engineering Research Council
[17] Supported by the Minerva Gesellschaft für Forschung GmbH
[18] Supported by the US Department of Energy, contract DE-AC02-76ER00081 and by the U.S. National Science Foundation Grant Number INT-8313994 for travel
[19] Supported by CAICYT

Abstract. Vector meson production is studied in the reaction $\gamma\gamma \to K^+ K^- \pi^+ \pi^-$. A clear $\Phi(1020)$ signal is seen in the $K^+ K^-$ mass distribution and a $K^{*0}(890)$ signal is visible in the $K^\pm \pi^\mp$ one. Both do not seem to be strongly correlated with quasi two body final states. Cross sections for the processes $\gamma\gamma \to K^+ K^- \pi^+ \pi^-$, $\gamma\gamma \to \Phi\pi^+\pi^-$, $\gamma\gamma \to K^{*0} K^\pm \pi^\mp$ and upper limits for the production of $\Phi\rho$, $\Phi\Phi$ and $K^{*0}\overline{K^{*0}}$ are given as function of the invariant $\gamma\gamma$ mass.

I. Introduction

The study of vector meson production in $\gamma\gamma$ collisions is motivated by the attempt to understand the origin of the large cross section for the reaction $\gamma\gamma \to \rho^0\rho^0$ near threshold [1, 2]. This cross section is roughly an order of magnitude higher than one would obtain from pomeron exchange within VDM (vector dominance model).

Several models have been suggested to explain this result: a) Production of a resonance (or a glueball) which decays to a $\rho\rho$ pair [3]. These models are partly inconsistent with the spin-parity structure of the $\rho^0\rho^0$ system seen in the data [1] and with a lack of signal in the $\rho^+\rho^-$ final state [4]. b) A t-channel factorization treatment which relates two-photon processes to photoproduction and data of hadronic reactions [5, 6]. This model predicted [5] a large cross section for the production of $\omega\omega$ and $\rho^0\omega$ pairs, in contrast to experimental results [7]. However recent revised calculations [6, 7] are not inconsistent with the data. c) Production of interfering $I=0$ and $I=2$ four-quark bound states [8–10], based on the static version of the MIT bag model [11]. These models are not in contradiction with the experimental results.

Additional information on vector meson pair production in $\gamma\gamma$ collisions is thus crucial for the understanding of the $\rho^0\rho^0$ effect and in order to confirm or reject the exotic interpretation as $q\bar{q}q\bar{q}$ states. In this paper we look for the production of the vector mesons containing strange quarks, $\phi(1020)$ and $K^{*0}(892)$, both inclusively and as vector meson pairs.

II. Event Selection

In this paper we report on vector meson production in the reaction

$$e^+e^- \to e^+e^- K^+ K^- \pi^+ \pi^- \qquad (1)$$

observed with the TASSO detector at PETRA, at beam energies E_b between 7 and 18 GeV. A description of the detector can be found elsewhere [12]. No requirement has been made on the detection of the scattered e^+ and e^- in the final state. The data sample corresponds to an integrated luminosity of $\approx 72\ \text{pb}^{-1}$ with most of the data taken around $E_b = 17$ GeV.

The trigger imposed one of the following requirements [1, 13]: (i) at least two tracks separated by more than 154° in azimuth, with associated signals in the inner time-of-flight (TOF) counters, or (ii) two or more tracks originating from the interaction region within ± 15 cm along the beam direction, or (iii) four or more tracks. The tracks are measured in the central detector. The trigger efficiency per track varied as a function of the track momentum component (p_t) transverse to the beam direction. For most of the data this efficiency was about 50% for tracks with $p_t \approx 0.17$ GeV/c, rising to 95% for $p_t \geqq 0.29$ GeV/c.

Event candidates for reaction (1) produced via two-photon collisions are selected by requiring exactly four acceptable tracks with net charge zero, where the definition of an acceptable charged particle is given in [14]. In order to suppress background from one-photon annihilation events, the sum of the measured charged particle momenta had to be less than 8 GeV/c. Beam-gas interactions are reduced by requiring $|z_v| < 8$ cm, where z_v is the coordinate along the beam axis of the event measured by averaging over the tracks. Two-photon events with undetected particles are suppressed by demanding the vector sum of the transverse momenta of the four particles, $|\sum \mathbf{p}_t|$, to be less than 0.12 GeV/c. The data sample after these cuts contains 5,374 events, and is dominated by the final state $\rho^0\rho^0$[1].

Another potential background to reaction (1) which may affect in particular the $\phi \to K^+ K^-$ search, is $\gamma \to e^+e^-$ conversions, which have similar kinematic characteristics (a small Q value) as the ϕ meson. For each pair of tracks a quantity $\phi_c = 1.075\ \text{GeV} - 0.5 \cdot M(e^+e^-)$ is defined, where $M(e^+e^-)$ is the invariant mass of the pair (in GeV) when the two particles are assumed to be electrons. When all pairs in which $M(K^+K^-) < \phi_c$ are rejected, the background from pair conversion is strongly reduced.

III. Particle Identification

Particle identification in reaction (1) is achieved by using TOF measurements. The TOF system consists of 48 scintillation counters surrounding the cylindrical drift chamber at a radial distance of 1.32 m from the beam axis. The polar angle covered by the TOF counters is approximately $|\cos\theta| < 0.82$. The typical time resolution of the system is 445 ps for particles

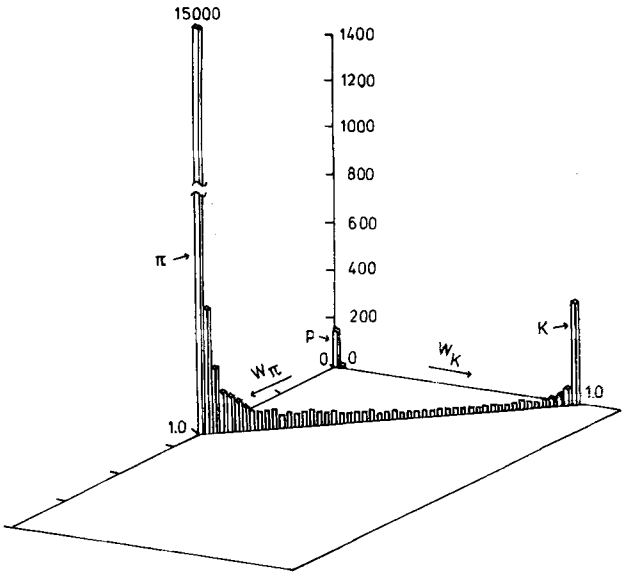

Fig. 1. Scatter plot of the kaon weight vs the pion weight of the tracks in the four prong sample with the cut $|\sum \mathbf{p}_t| < 0.12$ GeV/c

passing through the center of the counters, improving linearly to 265 ps for particles passing close to either end. The efficiency of the TOF measurement, averaged over the full period of data taking, was 92%. A π/K separation with the TOF counters has been attempted for momenta $P<1$ GeV/c and a (π or K)/p separation for momenta $P<1.4$ GeV/c.

For each track which has TOF information, the square of the mass (M^2_{TOF}) is computed from the measured track length, momentum and TOF values. Three Gaussian weights W_i are calculated for each particle type i ($i=\pi, K, p$) according to $W_i \sim \exp(-(\tau_m-\tau_i)^2/2\sigma_\tau^2)$, where τ_m is the measured TOF, τ_i the expected TOF for particle hypothesis i, and σ_τ is the r.m.s. resolution for the measured TOF. The three W_i's are normalized for each track such that $\sum W_i = 1$. For the highest W_i of each track, the difference $\Delta t = |\tau_m - \tau_i|$ is required to be less than 3 σ_τ. With the cut of $|\sum \mathbf{p}_t| < 0.12$ GeV/c, 85% of all particles in the sample have useful TOF measurements. A clear separation between π, K and p's is obtained with the above procedure, as can be seen in Fig. 1.

A track is defined as an identified π if $W_\pi > 0.5$ and $P<1$ GeV/c; as an identified K if $W_K > 0.95$ and $P<1$ GeV/c and $0.1 < M^2_{\mathrm{TOF}} < 0.6$ GeV^2; and as an identified p if $W_p > 0.95$ and $P<1.4$ GeV/c and $M^2_{\mathrm{TOF}} > 0.6$ GeV^2. A track is defined as *consistent* with being a pion (kaon, proton) if it is *not* an identified K or p(π or p; π or K). With these definitions $\approx 94\%$ of all particles with useful TOF measurement are identified as π, K or p.

IV. Monte-Carlo Simulation

The cross sections for reaction (1) and its sub-processes are evaluated by using Monte Carlo (MC) simulation programs. The full kinematics of the $\gamma\gamma$ system is generated according to the flux of transverse photons, using the exact formula from [15]. Isotropic phase space models are used to generate the final states $K^+K^-\pi^+\pi^-$, $\phi\pi^+\pi^-$, $\phi\rho^0$, $\phi\phi$, $K^{*0}K^{\mp}\pi^{\pm}$ and $K^{*0}\bar{K}^{*0}$. Resonances are allowed to decay into the relevant products ($\phi \to K^+K^-$, $\rho \to \pi^+\pi^-$, $K^{*0} \to K^{\pm}\pi^{\mp}$). All generated particles are passed through a full detector simulation program which includes trigger, detector resolution, multiple scattering, nuclear interactions, decays and energy loss in the beam pipe. Special attention is given to the simulation of the TOF system. The generated events are required to pass the same cuts imposed on the data.

V. Production of the Vector Meson $\phi(1020)$

Two samples are used for the extraction of a ϕ signal in its K^+K^- decay mode: 1) All K^+K^- invariant mass combinations are taken where both particles are consistent with being kaons ("K-consistent" sample). The rejection of combinations which contain identified pions is found to reduce significantly both the γ conversions and the $\rho^0\rho^0$ contamination. 2) Same as above, but at least one kaon is required to be an identified kaon, *or* both kaons are identified, but the weight requirement is relaxed such that all combinations with $W_{K^+} \cdot W_{K^-} \geqq 0.3$ are accepted ("identified K" sample). The first method yields higher statistics but has a larger background, whereas the second one is cleaner, but it suffers from limited statistics.

The "K-consistent" sample contains 1379 possible K^+K^- pair combinations. The invariant mass of each pair is computed and the spectrum is shown in Fig. 2a. A peak is seen in the region of the ϕ mass. No enhancement is seen in the $K^{\pm}K^{\pm}$ mass distribution or in the distribution of identified pion pairs with opposite charges, interpreted as kaons.

The K^+K^- distribution is fitted to a Gaussian-shaped resonance with the nominal ϕ mass value (1.02 GeV) plus a background (parametrized in terms of a second order polynomial multiplying the K^+ momentum in the K^+K^- rest frame), as shown in Fig. 2a (solid line). The fit yields 39 ± 10 ϕ's and the experimental width of the ϕ signal (0.016 GeV) is consistent with the resolution obtained in the MC generation.

The "identified K" sample contains 444 K^+K^- combinations and the spectrum is shown in Fig. 2b. A clean ϕ signal is seen. A similar fit as described above (with a first order polynomial, which describes

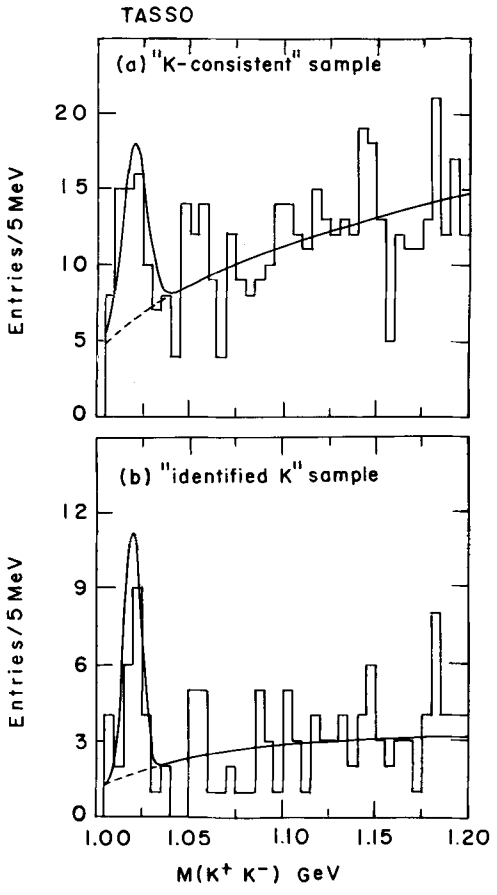

Fig. 2. a Invariant mass distribution of the K^+K^- system for the "K-consistent" sample. Fit is Gaussian resonance plus background (see text). **b** Same as **a** for the "identified K" sample

well the background shape) is given for this distribution, yielding 20.3 ± 4.4 ϕ's, and again the width (0.010 GeV) is consistent with the MC resolution.

The cross section of the reaction

$$\gamma\gamma \to \phi \pi^+ \pi^- \tag{2}$$

is calculated as a function of the $\gamma\gamma$ invariant mass, $W_{\gamma\gamma}$, from fits similar to those of Fig. 2, using MC generated events. No TOF information is used for the pair of particles recoiling against the ϕ in reaction (2) and both are assumed to be pions.

In order to estimate the leakage of high multiplicity events into the ϕ sample with the cut of $|\sum \mathbf{p}_t| < 0.12$ GeV/c, we show in Fig. 3a the $(\sum \mathbf{p}_t)^2$ distribution of events (without the $|\sum \mathbf{p}_t|$ cut) from the "K-consistent" sample of reaction (2) where ϕ is defined as $M(K^+K^-) < 1.03$ GeV. The points with error bars (statistical only) are data and the solid curve is the result of a fit of the data to the MC distribution for reaction (2) plus a flat distribution to account

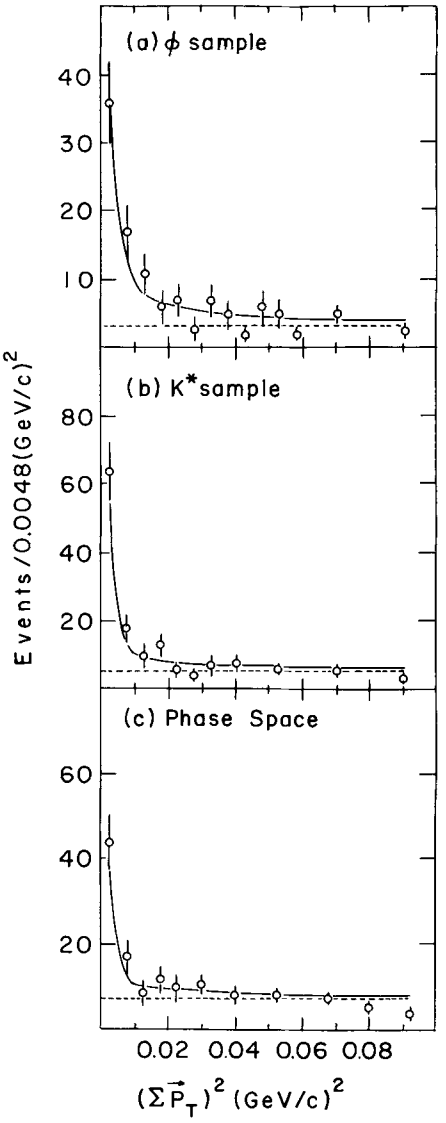

Fig. 3a–c. The $|\sum \mathbf{p}_t|^2$ distributions for the reactions $\gamma\gamma \to \Phi\pi^+\pi^-$, $\gamma\gamma \to K^{*0}K^{\mp}\pi^{\pm}$ and $\gamma\gamma \to K^+K^-\pi^+\pi^-$ phase space, respectively

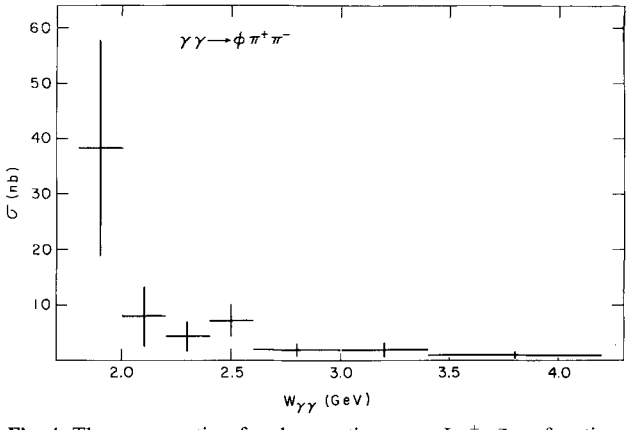

Fig. 4. The cross section for the reaction $\gamma\gamma \to \Phi\pi^+\pi^-$ as function of $W_{\gamma\gamma}$. The errors are statistical only

Table 1. Cross sections of the various subprocesses of reaction (1) and fractions of the topological cross section as a function of $W_{\gamma\gamma}$

$W_{\gamma\gamma}$(GeV)	$\gamma\gamma \to \phi\pi^+\pi^-$		$\gamma\gamma \to K^{*0}K^{\mp}\pi^{\pm}$		$\gamma\gamma \to K^+K^-\pi^+\pi^-$ P.S.		$\gamma\gamma \to K^+K^-\pi^+\pi^-$ top.
	σ(nb)	fraction of σ(top)%	σ(nb)	fraction of σ(top)%	σ(nb)	fraction of σ(top)%	σ(nb)
1.8–2.0	38 ±19	44±22	34 ±18[a]	41±24	6.6±3.0	15± 7	43 ±14.4
2.0–2.4	5.8± 2.7	11± 5	23 ± 5.5	57±14	8.8±1.9	32± 7	27 ± 4.3
2.4–2.8	4.4± 1.5	15± 5	3.0± 3.9	14±18	10.4±2.1	71±14	14.5± 3.4
2.8–3.4	2.0± 0.9	22±10	1.8± 2.5	26±38	2.3±1.0	52±22	4.4± 2.0
3.4–4.2	0.9± 0.5	39±21	–	–	0.7±0.7	61±62	1.2± 0.8

[a] Sum of $K^*K\pi$ and $K^*\overline{K^*}$ production (see text)

for the leakage of the high multiplicity events. We estimate a background of (14±2)% of high multiplicity events in our "K-consistent" sample. No $W_{\gamma\gamma}$ dependence of this correction can be seen, and we apply it as an overall correction.

In Fig. 4 the cross section of reaction (2), corrected for all ϕ decay modes, is presented as a function of $W_{\gamma\gamma}$ for the "K-consistent" sample. The errors are statistical only. Systematic errors of ≈30% are due to uncertainties in the background parametrization (≈25%) and in the acceptance and overall normalization (≈18%). The cross section is falling from ≈20 nb at $W_{\gamma\gamma}=2$ GeV to ≈1 nb at $W_{\gamma\gamma}=4$ GeV. These cross sections are also given in Table 1. An analysis of the "identified K" sample yields similar results within errors.

In order to search for possible $\phi\rho^0$ and $\phi\phi$ signals, the invariant mass distributions of the pair of particles recoiling against the ϕ (as defined above) has been plotted. For the $\phi\rho^0$ search, the recoiling particles were assumed to be pions, while for the $\phi\phi$ search they were required to be consistent with kaons. No evidence is seen for a ρ^0 signal in the data, and no "K^+K^-" combinations recoiling against the ϕ appear in the region $M(\text{"}K^+K^-\text{"}) < 1.08$ GeV.

Upper limits (95% C.L. including a systematic error of 30%) for the cross sections of the reactions $\gamma\gamma \to \phi\rho^0$ and $\gamma\gamma \to \phi\phi$ are given in Fig. 5a–b. Predictions for the cross sections of the processes $\gamma\gamma \to q\bar{q}q\bar{q} \to \phi\rho^0$ and $\gamma\gamma \to q\bar{q}q\bar{q} \to \phi\phi$ have been given by various authors using four-quark models [8–10]. The experimental results are not in contradiction with most of the predictions for the existence of such states. However, the highest curve of [9] can be ruled out in the combined region of $2.0 < W_{\gamma\gamma} < 2.6$ GeV. Experimentally our upper limit for this region is 8.7 nb, and in the $\phi\phi$ case, for the region $2.2 < W_{\gamma\gamma} < 3.0$ GeV, it is 1.4 nb (95% C.L.). The results are also consistent with the t-channel exchange model of [6].

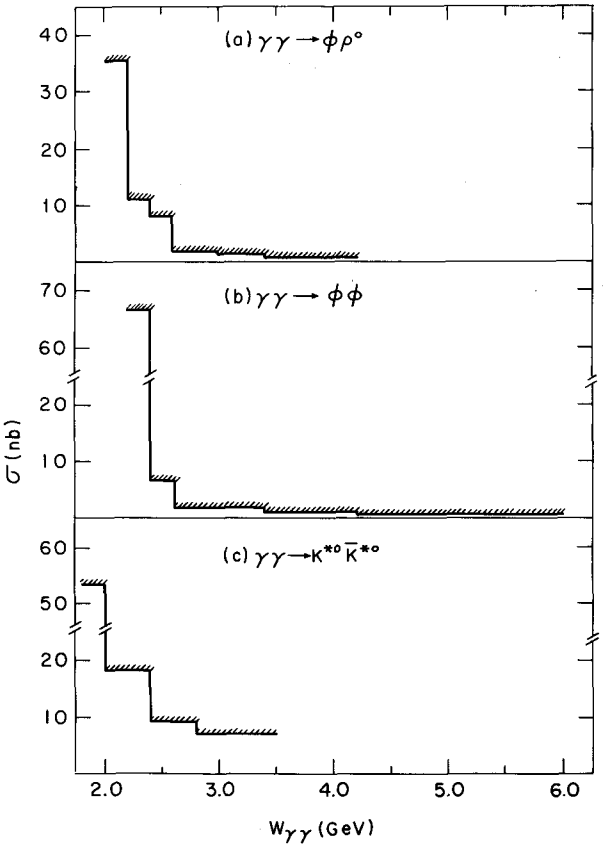

Fig. 5a–c. Upper limits (95% C.L.) as function of $W_{\gamma\gamma}$ for the final states **a** $\Phi\rho$, **b** $\Phi\Phi$, **c** $K^{*0}\overline{K^{*0}}$

VI. Production of the Vector Meson $K^*(892)$

The extraction of the ϕ cross section in reaction (2) is relatively straight-forward, since the ϕ is a narrow resonance situated near the beginning of the K^+K^- phase space distribution and thus has a small background. In fact the ϕ is clearly visible even without requiring K-identification or when requiring one iden-

tified-K (see Fig. 2). This is not the case for the $K^{*0}(892)$, which is a wider resonance and sits at the peak of the phase space distribution of reaction (1). Moreover, a study of $\rho^0\rho^0$ MC events shows that there is a kinematical overlap between the $\rho^0\rho^0$, which is copiously produced in the four-prong sample, and the K^{*0} (assigning to the same particle π and K masses respectively).

In order to extract a clean K^* signal from the reaction

$$\gamma\gamma \to K^{*0} K^{\mp} \pi^{\pm} \tag{3}$$

where the K^{*0} decays into $K^{\pm}\pi^{\mp}$, severe cuts must be applied concerning in particular the K identification and the possible reflection of the $\rho^0\rho^0$ final state. Thus the K and π identification criteria are chosen to be much stricter: a track is called an identified K only if its W_K is larger than 0.99 and an identified π only if $W_\pi > 0.9$. The other conditions mentioned in Sect. III are unchanged.

In order to minimize the non-K background for the K^{*0} search we restrict ourselves to a sample in which at least one K and one oppositely charged π are identified. There are 287 such events with 426 identified $K^{\pm}\pi^{\mp}$ combinations:

$$\gamma\gamma \to K_1^{\pm} \pi_2^{\mp} K_3^{\mp} \pi_4^{\pm}. \tag{4}$$

In (4) particles 1 and 2 are the identified ones while no cuts are imposed on particles 3 and 4. In genuine candidates for reaction (1), particle 3 must be a K and particle 4 a π. However, in addition to these candidates, the above sample includes three types of background not due to genuine $K^+K^-\pi^+\pi^-$ events: a) Leakage of high multiplicity events to the $|\sum \mathbf{p}_t| < 0.12$ GeV/c region; b) contribution of the final state $K^{\pm}\pi^{\mp}K_S^0$; $K_S^0 \to \pi^+\pi^-$; c) contamination of non-K background in the identified-K sample, mainly originating from the dominant $\rho^0\rho^0$ final state.

The M^2_{TOF} distribution of particles 3 and 4 are shown in Fig. 6a–b for those particles which have useful TOF measurements (356 and 361 respectively, from the above 426 combinations). A K peak, well separated from the pions, is clearly visible in Fig. 6a (also when one repeats the plots in several $W_{\gamma\gamma}$ bins), while no such peak is seen in Fig. 6b, as expected. The number of entries in the M^2_{TOF} regions of the π and K in both plots are consistent with the expected contributions from the genuine $K^+K^-\pi^+\pi^-$ events plus the above mentioned types of background. From Fig. 6a it is obvious that in order to obtain a clean sample of reaction (1) one must remove the pions from K_3.

The final sample for the study of reaction (3) is obtained by removing all ϕ candidates ($M(K^+K^-) <$ 1.03 GeV) and imposing the condition that K_3 in (4) be a consistent K, thus removing identified pions and keeping only identified and consistent kaons. Similarly π_4 is required to be a consistent π. This sample consists of 162 events, out of which $(67 \pm 5)\%$ are estimated to be genuine $K^+K^-\pi^+\pi^-$ events and the rest originate from the three types of background discussed above. The average K identification probability in this final sample is about 56%, in agreement with MC calculations.

The distribution of $M(K^{\pm}\pi^{\mp})$ for this sample (2 combinations/event) is shown in Fig. 7. A K^{*0} signal is seen on top of some background. No such en-

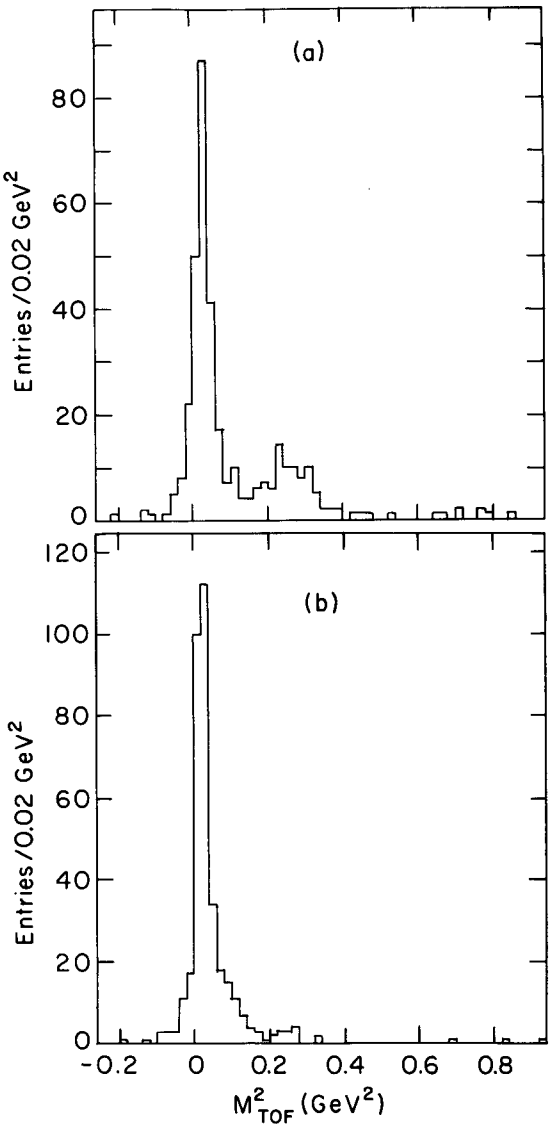

Fig. 6a, b. M^2_{TOF} distribution for particles recoiling against the identified $K^{\pm}\pi^{\mp}$ system in reaction (4) (see text): **a** expected kaons, **b** expected pions

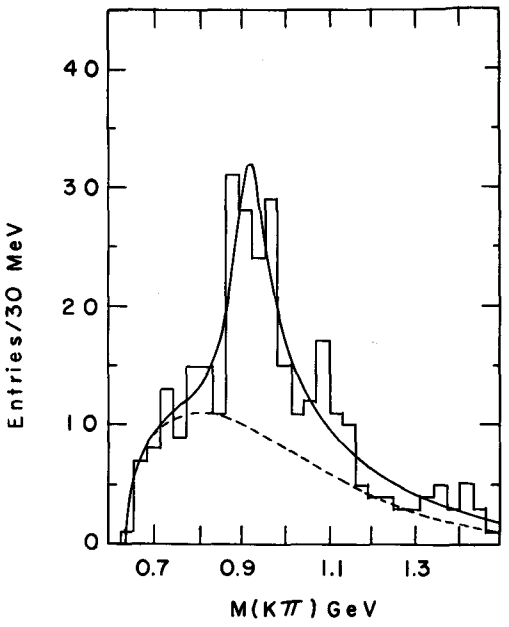

Fig. 7. Invariant mass distribution of the identified $K^{\pm}\pi^{\mp}$ system in the final sample of 162 events (see text). The solid curve is a fit to a relativistic Breit-Wigner resonance plus background (dashed curve) parametrized by the shape of the same sign $K\pi$ distribution multiplying a threshold phase space factor (see text)

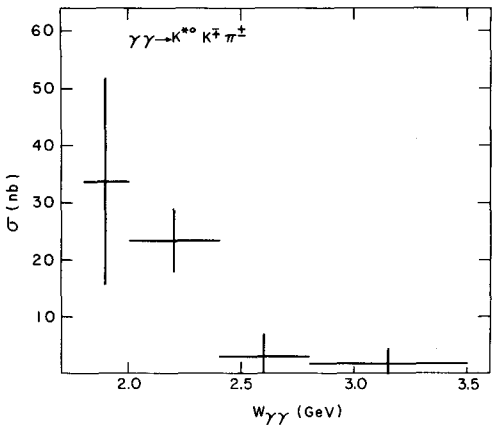

Fig. 8. The cross section for the reaction $\gamma\gamma \to K^{*0}K^{\pm}\pi^{\mp}$ as function of $W_{\gamma\gamma}$. The errors are statistical only

hancement is seen when same sign invariant mass combinations $M(K^{\pm}\pi^{\pm})$ are plotted.

The distribution of Fig. 7 has been fitted to a relativistic P-wave Breit-Wigner shaped resonance with free mass and width values plus a background. The parametrization of the background was obtained from fitting the same sign $M(K^{\pm}\pi^{\pm})$ distribution to a second order exponential multiplying a phase space threshold factor (given by the $K^{\pm}$ momentum in the $K^{\pm}\pi^{\pm}$ rest frame). A good fit ($P(\chi^2)=0.62$) is obtained, yielding 126 ± 34 K^{*0}'s, a mass of 0.927 GeV and a width of 0.128 GeV. The width obtained from the MC generated events after convoluting the experimental resolution with the natural K^* width is 0.070–0.075 GeV. The fitted mass and width values are somewhat higher than expected for the K^*; however, the goodness of fit obtained by fixing the mass and width to the PDG [16] and MC values respectively ($M=0.892$ GeV; $\Gamma=0.071$ GeV) is comparable with the previous one ($P(\chi^2)=0.25$), and it yields 89 ± 17 K^{*0}'s. Note also that by using as background the shape of the $M(K^{\pm}\pi^{\mp})$ distribution from the $K^+K^-\pi^+\pi^-$ MC, similar results are obtained with 114 ± 36 K^{*0}'s and fitted K^* mass and width values of 0.910 and 0.095 GeV respectively. Repeating the same procedure for the more restricted sample of about 70 events, where the M^2_{TOF} of the recoiling K_3 is in the K-meson range (0.14–0.60 GeV), we obtain essentially the same results, with $M(K^*)=0.906$ GeV, and a number of K^*'s corresponding to the smaller sample.

The cross section for reaction (3) has been calculated as a function of $W_{\gamma\gamma}$ from fits similar to those of Fig. 7, with the K^* mass and width fixed to the above mentioned PDG and MC values. As in the ϕ case, the background from undetected particles in the K^* sample (defined by $0.86<M(K^{\pm}\pi^{\mp})<0.98$ GeV), with the cut on $|\sum \mathbf{p}_t|<0.12$ GeV/c, is estimated from the $(\sum \mathbf{p}_t)^2$ distribution of the K^* events, shown in Fig. 3b. Repeating the same procedure as for the ϕ, we estimate this background to be $(16\pm3)\%$ and subtract it accordingly. The cross sections have been calculated both by the above procedure and also from a two-dimensional fit of the scatter plot $M(K^+\pi^-)$ vs $M(K^-\pi^+)$ to a sum of contributions from $K^+K^-\pi^+\pi^-$, $K^*K\pi$ and $K^*\overline{K^*}$ final states. Similar results are obtained by the two methods in all $W_{\gamma\gamma}$ bins except for the first one ($W_{\gamma\gamma}=1.8$–2.0 GeV), where the two-dimensional fit yields some contribution of $K^*\overline{K^*}$.

In Fig. 8 the cross sections of reaction (3), corrected for all K^{*0} decay modes, are given as a function of $W_{\gamma\gamma}$ with statistical errors only. The systematic errors are similar to the $\phi\pi\pi$ case. For all $W_{\gamma\gamma}$ bins except for the first one, the results are taken from the one-dimensional fits, which have a better statistical accuracy. For the first bin the two-dimensional fit is more trustworthy, because of the limited available phase-space which causes overlap of the various final states, and the indications for $K^*\overline{K^*}$ production. The fit yields in this $W_{\gamma\gamma}$ region $(29\pm16)\%$ of double K^* production, corresponding to a cross section of (23 ± 13) nb. The cross section given in Fig. 8 for the first $W_{\gamma\gamma}$ bin is the sum of both contri-

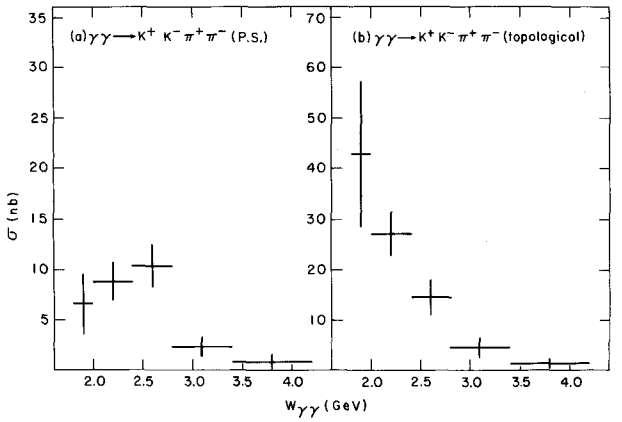

Fig. 9a, b. The cross section for the reaction $\gamma\gamma \to K^+ K^- \pi^+ \pi^-$ as function of $W_{\gamma\gamma}$. The errors are statistical only. **a** Non-resonant phase space cross section. **b** Total topological cross section

butions to K^* production i.e. $K^* K\pi$ and $K^* \overline{K^*}$. The cross section falls from ≈ 30 nb at $W_{\gamma\gamma} = 2.0$ GeV to about 2 nb at $W_{\gamma\gamma} = 3.2$ GeV. Table 1 also summarizes these cross sections.

The search for a possible $K^{*0} \overline{K^{*0}}$ signal was performed by the above-mentioned two-dimensional fits and also from the invariant mass distribution of the pair of particles $K^{\mp}\pi^{\pm}$ recoiling against the $K^{*0} \to K^{\pm}\pi^{\mp}$ (as defined above). The $K^{\mp}$ ($\pi^{\pm}$) was required to be consistent with a kaon (pion) hypothesis. The two methods give the following consistent results: No evidence for $K^{*0} \overline{K^{*0}}$ production is seen for all $W_{\gamma\gamma}$ bins except for the first one, where a signal of almost 2 s.d. is apparent, as discussed above. Since the $K^* \overline{K^*}$ signal in this bin is barely significant, we present it only as an upper limit together with the other $W_{\gamma\gamma}$ bins. In Fig. 5c, the 95% C.L. upper limits (including a systematic error of 30%) for the cross section of the reaction $\gamma\gamma \to K^{*0} \overline{K^{*0}}$ are given. As for the $\phi\rho^0$ and $\phi\phi$, the results are not inconsistent with the prediction [8] of four quark states decaying into $K^* \overline{K^*}$.

VII. Cross Sections for $\gamma\gamma \to K^+ K^- \pi^+ \pi^-$

In order to obtain the cross section for the non-resonance phase space final state $K^+ K^- \pi^+ \pi^-$, events with ϕ or K^{*0} signals, as defined above, are removed, and the $W_{\gamma\gamma}$ distribution of the remaining events (70 out of the above 162 events) is compared with the MC results.

The cross section for the non-resonant reaction $\gamma\gamma \to K^+ K^- \pi^+ \pi^-$ is shown in Fig. 9a as a function of $W_{\gamma\gamma}$. The backgrounds from undetected particles within the cut $|\sum \mathbf{p}_t| < 0.12$ GeV/c ($(30 \pm 3)\%$, see Fig. 3c) and from the K^0_S and π contamination in the identified-K sample ($(10 \pm 4)\%$) have been subtracted. The errors are statistical only. Systematic errors are estimated to be $\approx 25\%$ and are mainly due to the particle identification procedure, and uncertainties in the acceptance and overall normalization. The cross section is about 10 nb up to $W_{\gamma\gamma} = 2.6$ GeV, and then falls to about 1 nb at $W_{\gamma\gamma} = 4.0$ GeV.

The overall topological cross section of the reaction $\gamma\gamma \to K^+ K^- \pi^+ \pi^-$, which is the sum of the non-resonant phase space final state, the reaction $\gamma\gamma \to \phi\pi^+\pi^-$, $\phi \to K^+ K^-$, and the reaction $\gamma\gamma \to K^{*0} K^{\mp}\pi^{\pm}$, $K^{*0} \to K^{\pm}\pi^{\mp}$, is shown as a function of $W_{\gamma\gamma}$ in Fig. 9b. Errors are as in Fig. 9a. The first bin includes also the $K^* \overline{K^*}$ contribution, as discussed above. The cross section falls monotonically from ≈ 35 nb at $W_{\gamma\gamma} = 2$ GeV to ≈ 1 nb at $W_{\gamma\gamma} = 4$ GeV. A summary of the topological and the various channel cross sections is given in Table 1. It is interesting to note from Table 1 that as in the 4π final state [1], also here resonance production dominates the topological cross section at low $W_{\gamma\gamma}$.

VIII. Conclusions

The reaction $\gamma\gamma \to K^+ K^- \pi^+ \pi^-$ has been studied in the TASSO detector by using momentum and TOF measurements. The topological cross section is falling with $W_{\gamma\gamma}$ from ≈ 35 nb at 2 GeV to ≈ 1 nb at 4 GeV. A $\phi(1020)$ signal is seen in the three-body final state $\phi\pi^+\pi^-$, with cross sections of ≈ 20 nb at $W_{\gamma\gamma} =$ 2 GeV and of ≈ 1 nb at $W_{\gamma\gamma} = 4$ GeV. Significant $K^{*0}(892)$ production occurs in the three-body final state $K^{*0} K^{\mp}\pi^{\pm}$ (≈ 30 nb at $W_{\gamma\gamma} = 2.0$ GeV and ≈ 2 nb at $W_{\gamma\gamma} = 3.2$ GeV). The ϕ and K^* production are not dominated by the quasi two body final states $\phi\rho^0$, $\phi\phi$ and $K^{*0} \overline{K^{*0}}$. Upper limits for these processes are not in contradiction with most predictions of four-quark states or t-channel factorization estimates. No quantitative predictions are available to explain the production of the final states $\phi\pi^+\pi^-$ and $K^{*0} K^{\mp}\pi^{\pm}$, which have also been reported in [17]. In particular, contrary to vector mesons like the ϕ, K^*'s are less naturally produced in $\gamma\gamma$ collisions, since they are not directly coupled to photons.

Acknowledgements. We gratefully acknowledge the support of the DESY directorate and the PETRA machine group. Those of us from abroad wish to thank the DESY directorate for the hospitality extended to us while working at DESY. We thank Dr. D. Hochman for help in the fits and Mr. A. Yagil for help in the generation of the Monte-Carlo events.

References

1. TASSO Collab. R. Brandelik et al.: Phys. Lett **97B**, 448 (1980); M. Althoff et al.: Z. Phys. C – Particles and Fields **16**, 13 (1982)
2. D.L. Burke et al.: Phys. Lett. **103B**, 153 (1981); H.J. Behrend et al.: Z. Phys. C – Particles and Fields **21**, 205 (1984)
3. H. Goldberg, T. Weiler: Phys. Lett. **102B**, 63 (1981)
4. H. Kolanoski: Proc. 5th Int. Workshop on Photon Photon Collisions, Aachen, Ed., Ch. Berger, p. 175. Lect. Notes Phys. 191. Berlin, Heidelberg, New York: Springer 1983
5. G. Alexander, U. Maor, P.G. Williams: Phys. Rev. **D26**, 1198 (1982)
6. G. Alexander, A. Levy, U. Maor: Z. Phys. C – Particles and Fields **30**, 65 (1986)
7. PLUTO Collab. Ch. Berger et al.: Z. Phys. C – Particles and Fields **29**, 183 (1985)
8. N.N. Achasov, S.A. Devyanin, G.N. Shestakov: Phys. Lett. **108B**, 134 (1982); Z. Phys. C – Particles and Fields **16**, 55 (1982)
9. N.N. Achasov, S.A. Devyanin, G.N. Shestakov: Z. Phys. C – Particles and Fields **27**, 99 (1985)
10. B.A. Li, K.F. Liu: Phys Lett. **118B**, 435 (1982); Phys. Rev. **D30**, 613 (1984)
11. R.L. Jaffe, K. Johnson: Phys. Lett. **60B**, 201 (1976); R.L. Jaffe: Phys. Rev. **D15**, 267 and 281 (1977)
12. TASSO Collab. R. Brandelik et al.: Phys. Lett. **83B**, 261 (1979); Z. Phys. C – Particles and Fields **4**, 87 (1980)
13. TASSO Collab. M. Althoff et al.: Phys. Lett. **121B**, 216 (1983); Phys. Lett. **142B**, 135 (1984)
14. TASSO Collab. R. Brandelik et al.: Phys. Lett. **113B**, 499 (1982)
15. V.M. Budnev et al.: Phys. Rep. **15**, 181 (1975)
16. Particle Data Group: Rev. Mod. Phys. **56**, 2(II) (1984)
17. TPC/Two-Gamma Collab. H. Aihara et al.: Phys. Rev. Lett. **54**, 2564 (1985)